J. Phys. A: Math. Gen. 27 (1994) 683–696. Printed in the UK

On the drift and diffusion of a rod in a lattice fluid

F J Alexander† and J L Lebowitz‡

† Center for Nonlinear Studies, Los Alamos National Laboratory, Los Alamos, New Mexico 87545, USA

‡ Departments of Mathematics and Physics, Rutgers University, New Brunswick, New Jersey 08903, USA

Received 24 June 1993

Abstract. We study the dynamics of a 'rod', a large particle which occupies several lattice sites, as it moves in a fluid of monomers each of which occupies only one site. Both the rod and the monomers move by hopping to unoccupied neighbouring sites, interacting with each other through a hard-core exclusion which prevents two particles from occupying the same site. Reversible hopping rates give rise to a diffusive process for the rod which, when rescaled, converges to standard Brownian motion. We use computer simulations to determine the diffusion coefficient as a function of rod size and monomer density. Non-reversible rates bias hops in one particular direction and give rise to a driven diffusive behaviour which shows a surprising relationship between the rod's velocity and its size [1]. Here we present a detailed description of this phenomenon including the case where the rod is held stationary, forming a fixed obstacle. We show that some of the features of this driven system can be accounted for by a discretized, Burgers-like equation whose linearized continuum analogue describes the flow of ground water past an obstacle, but more work remains to be done on the continuum limit of this model.

1. Introduction

In this paper we continue our investigations of a system first introduced in [1], to model segregation of different-sized particles subjected to shaking in a gravitational field, 'the Brazil nut effect' [2, 3]. The model consists of a gas of monomers and a single rod on a lattice. A monomer occupies one site and the rod more than one. The particles interact by hard-core exclusion; no more than one particle (of either type) is permitted per site. A monomer at site x waits for a Poisson-distributed time with mean 1 and then selects a lattice direction $\hat{e}$ with probability $p(\hat{e})$. If the neighbouring site $y = x + \hat{e}$ is unoccupied, the particle jumps to that site; otherwise it does not move.

The rod, just as with the monomers, also waits for a Poisson-distributed time with mean 1 and then selects a direction to attempt a hop according to the same rules. In particular, the rod can only move when there are enough empty sites to accommodate it. The dynamics of the rod complicates the analysis of this system (by breaking translation invariance), and therefore, to simplify matters as much as possible, we assume that we are on a two-dimensional square lattice, $\mathbf{Z}^2$, and that the rod is rigidly aligned in the vertical direction. For a rod of length L to move horizontally, all L sites immediately adjacent to it in the direction of motion must be simultaneously unoccupied. Vertical motion requires only that the *one* site adjacent in that direction be empty. This is illustrated in figure 1.

When there is no rod present, our model is just the much studied simple exclusion process whose stationary state is a product measure [4, 6]. When the exchange rates are symmetric, $p(\hat{e}) = p(-\hat{e})$, then the dynamics is just reversible Kawasaki dynamics, and the

0305-4470/94/030683+14$07.50

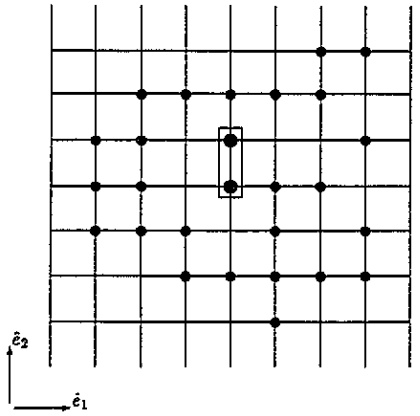

Figure 1. Rod dynamics. The rod ($L = 2$) may move down or to the left only.

stationary measure remains a Gibbs measure for a system of hard particles even with a rod present. It is easy to verify that the only correlations in this measure come from the direct hard-core exclusion of monomers from the sites occupied by the rod. This is so even for a finite density of rods as long as they all remain vertically aligned. When the exchange rates are not symmetric, however, the process is no longer reversible, and the Gibbs measure is no longer stationary under the dynamics. In particular, if we look at the distribution of monomers as seen from the rod, the density will be non-uniform and correlated.

We chose the asymmetry (driving field) to be perpendicular to the rod axis. Previous computer simulations [1] of this model showed a surprising relationship between the net velocity of the rod (average displacement in the field direction per unit time) and its length in the stationary state. Beyond a certain length (which depends on jump rates $p(\hat{e})$ and monomer density ρ_0), longer rods moved *faster*! This behaviour is certainly counter-intuitive, since we expect the exclusion rule to inhibit the motion of long rods more than that of short rods.

In this paper we study both the diffusive and driven versions of this model. In section 2 we show that when the jump rates are symmetric, the motion of the rod converges to Brownian motion. From computer simulations we determine the corresponding diffusion constant as a function of rod length. In section 3 we consider the driven, asymmetric case and present results of new, more comprehensive simulations. We also consider the case of a fixed rod corresponding to flow around an obstacle. We then show in section 4 that certain features of this system can be described well by a lattice Burgers' equation. A calculation of the density profile for weak asymmetry is given in the appendix.

2. Diffusion

In this section we consider symmetric jump rates: $p(\pm\hat{e}_1) = p(\pm\hat{e}_2) = \frac{1}{4}$. These give rise to purely diffusive motion. We examine three cases.

Single Particle. Consider the motion of a single particle, either a monomer or rod, with no other particles present on the lattice. This particle executes a simple random walk, and the resulting motion is diffusive with mean-square displacement $\langle(\Delta r)^2\rangle = D_0 t$, where

D_0 is the diffusion constant. Upon rescaling, this process converges to standard Brownian motion [5].

Tagged Monomer. Next consider the case of one tagged *monomer* in a 'sea of monomers' with density ρ_0; i.e. the rod with $L = 1$. The tagged particle is no longer able to execute a simple random walk because of the exclusion effects of the other monomers. One expects that the motion of the tagged particle is still diffusive, but with a reduced (ρ_0-dependent) diffusion constant $D(\rho_0)$. This is indeed the case, including convergence to Brownian motion, but it is by no means trivial to prove [6, 7].

As a first approximation one might expect that the diffusion constant is of the form $D(\rho_0) = D_0(1 - \rho_0)$, since successful jumps are reduced by a factor of $(1 - \rho_0)$ due to the exclusion rule; remember that ρ_0 is the density of monomers as seen from the tagged particle in the stationary state. This, however, involves an assumption that the tagged particle leaves no memory trace of its path. That is, each time the tagged particle attempts a jump, all neighbouring sites are occupied with *equal* probability ρ_0. What is clearly neglected is that when the tagged monomer jumps to a neighbouring site, then (obviously) the site just vacated is empty. Hence, the 'new neighbourhood' of the tagged monomer is not isotropic. Even though the vacated site may become occupied before the tagged particle attempts to jump again, it is more likely to be empty at the time of the next tagged monomer jump, and hence, the tagged monomer is more likely to return to it than to be at any other site. This, and other indirect 'correlation' effects reduce the diffusion constant even beyond that of the exclusion effect alone. To account for these effects the diffusion constant is commonly written as

$$D = D_0(1 - \rho_0) f(\rho_0) \tag{1}$$

where $f(\rho_0)$ is called the correlation factor.

The correlation factor has been studied theoretically in the context of solid state diffusion [8–10]. It has been calculated by perturbative methods and agrees well with computer simulations. On the two-dimensional square lattice [11] $D(\rho_0) = D_0(1-\rho_0)f(\rho_0)$, and the correlation factor is found to be given approximately by

$$f(\rho_0) \approx \frac{1 - \rho_0/2}{1 + 0.07\rho_0}. \tag{2}$$

Note that $f(\rho_0)$ in (2) equals 1 for $\rho_0 = 0$ and is a monotonically decreasing function of the density. In figure 2(*a*) we compare (2) to the correlation factor for a tagged monomer obtained from simulations. A similar comparison appears in [9].

For the symmetric simple exclusion process with arbitrary jump rates in two or higher dimensions, it is known that the self-diffusion matrix $\bar{S}(\rho_0)$ has the form $\bar{S}(\rho_0) = (1 - \rho_0)\bar{D}(\rho_0)$ where $\bar{D}(\rho_0)$ is non-decreasing in ρ_0. Moreover, $\bar{D}(\rho_0)$ is bounded away from zero from below as ρ_0 tends to 1 [12].

Diffusing Rod. When the rod has $L \geqslant 2$, the case of primary concern in this paper, then the diffusion constant for motion will also depend on the rod length. Since more sites need to be simultaneously unoccupied for the rod to move sideways, we expect and find that, for a fixed density of monomers, the diffusion constant in the x-direction decreases monotonically to zero with length. However, the correlation factor, now defined by

$$D_x = D_0(1 - \rho_0)^L f(\rho_0, L) \tag{3}$$

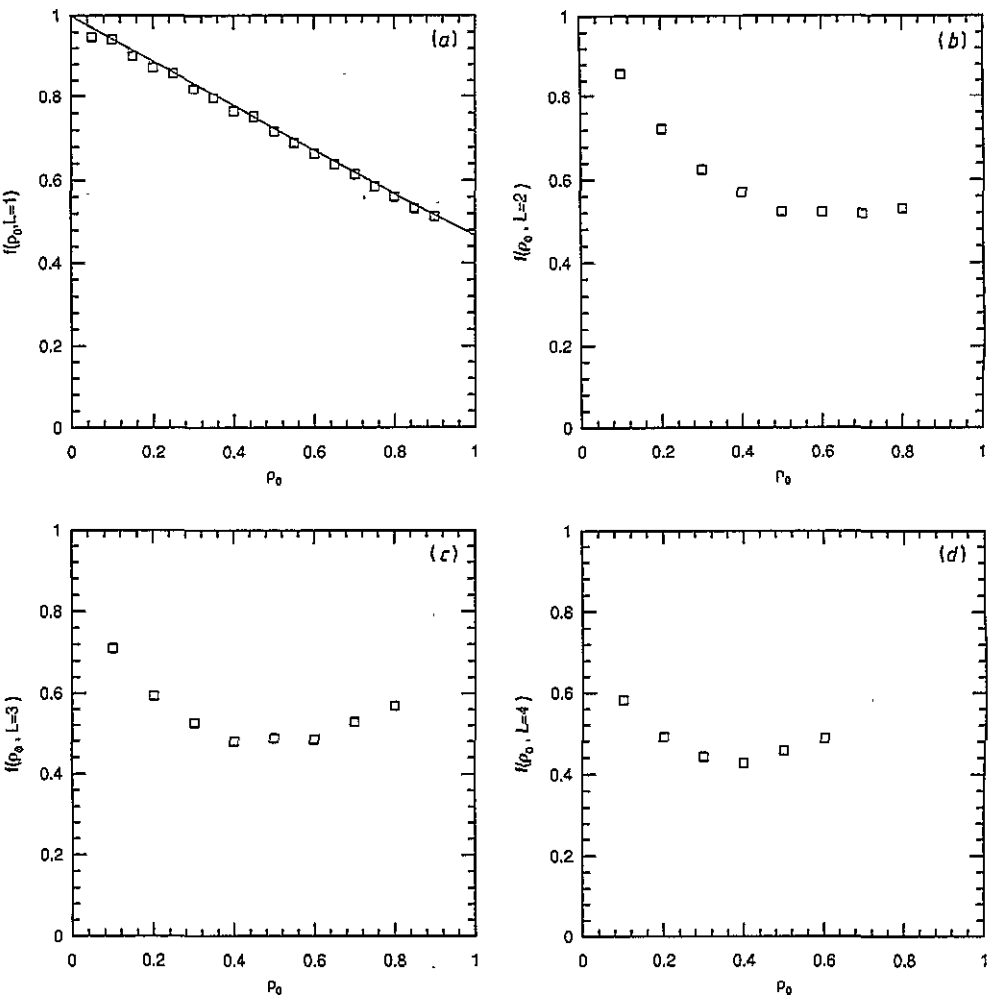

Figure 2. Correlation factors determined by simulating the diffusion process on lattices of size 16×16 with various monomer densities and tagged rod lengths. Averages were taken over an ensemble of 5000 independent systems. (*a*)–(*f*) Correlation factors for diffusion perpendicular to the rod axis. (*g*) Correlation factors for diffusion as a function of length for monomer densities $\rho_0 = 0.1$ (□), $\rho_0 = 0.3$ (•) and $\rho_0 = 0.5$ (◇).

has a more complicated behaviour. In particular, the correlation factor appears to be non-monotonic in the density ρ_0. Instead, there is a ρ_0 for which $f(\rho_0)$ has a minimum. This is shown in figures 2(*b*)–(*f*). In figure 2(*g*) we show the length dependence of the correlation factor for various densities. It appears, therefore, that at high densities, the rod is not as likely to return to the site that it has vacated as it is at lower densities. For longer rods, this 'critical density' decreases. The diffusion constant for motion parallel to the rod axis appears to be independent of length, to within statistical errors.

2.1. *Brownian motion*

We wish to show that under a proper rescaling of space and time the rod motion converges to

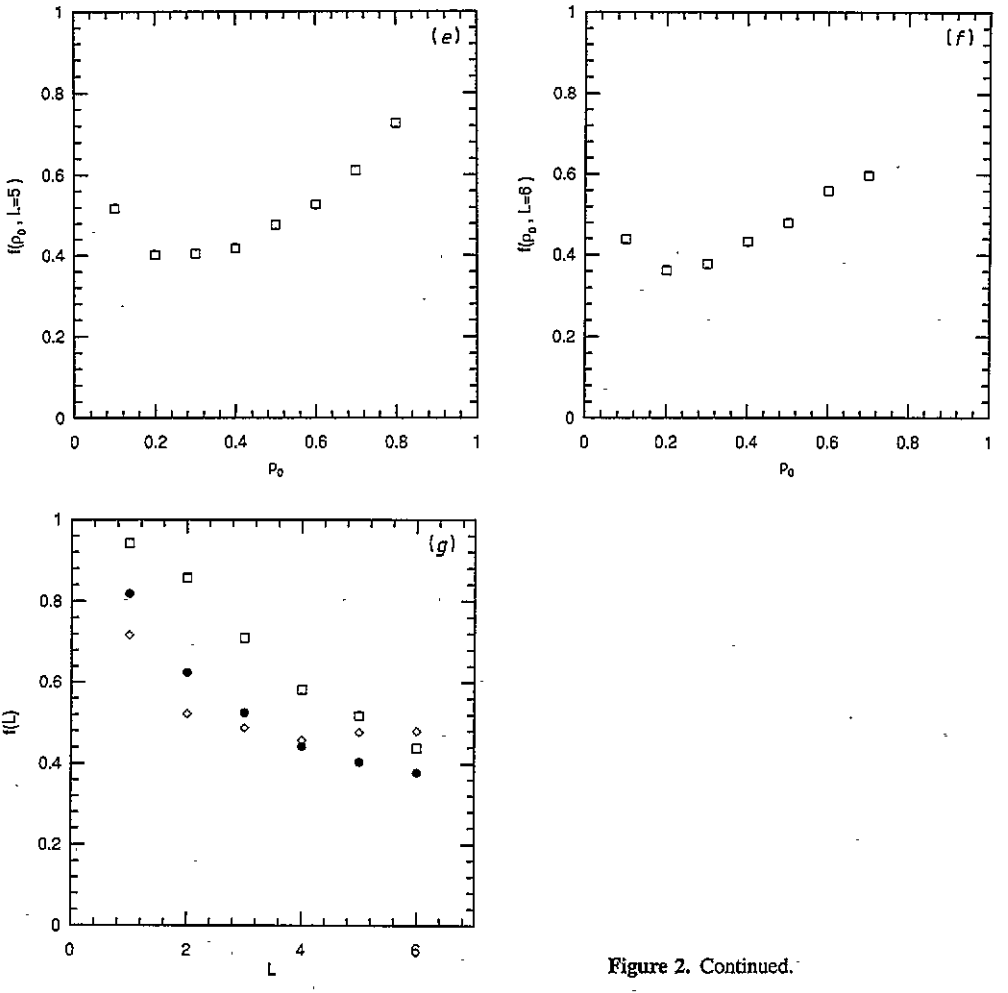

Figure 2. Continued.

Brownian motion with a positive diffusion constant, as was done by Kipnis and Varadhan [7] for a tagged monomer in a simple exclusion process.

Let x_t be the position of the rod at time t. For diffusive processes the length scale over which a particle diffuses is proportional to the square root of the time of evolution. We therefore look at the process on lengths rescaled by ϵ and times rescaled by ϵ^2. In the limit where $\epsilon \to 0$, the rescaled position of the rod, $x_t^\epsilon = \epsilon x_{\epsilon^{-2}t}$, should behave as a Brownian path.

To prove this, we observe that as already mentioned, the uniform product measure conditioned on having a rod at the origin, is a reversible measure for the dynamics as seen from the rod. It then follows from DeMasi *et al* [13] that the tagged particle motion converges to Brownian motion, and all we need to show is that the diffusion constant is strictly positive. We can do this by following Spohn's extension of the Kipnis–Varadhan argument [6], which then gives

$$\lim_{\epsilon \to 0} \epsilon x_{\epsilon^{-2}t} = (2\mathbf{D})^{1/2} b(t), \tag{4}$$

with $\mathbf{D} > 0$ a positive definite 2×2 matrix, and $b(t)$ a Brownian motion in two dimensions with $b(0) = 0$, and

$$\langle b_\alpha(t) b_\beta(t) \rangle = \delta_{\alpha\beta} \min(t, s) . \tag{5}$$

3. Driven system

For the case of asymmetric jump rates, we carried out simulations on $N \times N$ square lattices with periodic boundary conditions in both directions. On an initially empty lattice, we placed the rod with length $L = 1, 2, \ldots$ and then randomly deposited (the integer part of) $\rho_0(N^2 - L)$ monomers on the remaining sites subject to the exclusion rule. We simulated the process by randomly selecting a lattice site; if it was unoccupied, we chose another. Once an occupied site was selected, the particle at that location attempted to move to a neighbouring site as dictated by the probabilities $p(\hat{e})$:

$$p(-\hat{e}_1) = 0 \qquad p(\hat{e}_1) = b_\parallel \qquad p(-\hat{e}_2) = p(\hat{e}_2) = b_\perp = \tfrac{1}{2}(1 - b_\parallel) . \tag{6}$$

Next the occupancy of the target site was checked. If that site was empty, the move was successful, otherwise nothing happened, and the process repeated. This simulated the continuous-time Poisson process outlined above, and the jump rates guaranteed that the only conserved quantity was particle number.

For a pure monomer system we know the average velocity of a monomer exactly:

$$V(1, \rho_0) = b_\parallel (1 - \rho_0) . \tag{7}$$

Equation (7) follows from the fact mentioned earlier that a monomer sees a uniform distribution at density ρ_0, so that the probability that the site adjacent to the monomer is empty is $1 - \rho_0$. We compared simulations of these pure monomer systems to (7) and found for runs of 40 000 MCS that the simulated monomer velocities were typically within 1% of their exact values.

In figure 3 we plot the normalized velocity of the rod, defined as the ratio of the measured rod velocity to the known monomer velocity for the same parameters $V(L, \rho_0)/V(1, \rho_0)$ as a function of its length for three monomer densities $\rho_0 = 0.25$, 0.50 and 0.75. The lattice is of size 128×128 and the jump rates are $b_\parallel = 0.5$ and $b_\perp = 0.25$. As can be seen, there is a minimum in these curves, so longer rods move faster! How can this be, given that more sites need to be empty in order for the longer rods to move?

We considered the possibility that this anomaly was a result of finite lattice size. We found, however, that the 'longer rods travel faster' result was only *reinforced* by simulating the process on successively larger lattices. This behaviour is shown in figure 4 where we plot the velocity of an $L = 3$ and an $L = 6$ rod as a function of inverse lattice size. For these plots the density of monomers $\rho_0 = 0.5$ and the jump rates are as before. We allowed the system to evolve for 10 000 MCS to reach a stationary state, and over the next 40 000–50 000 MCS interval determined the rod velocity. These velocities for all but the largest $N = 256$ and $N = 512$ lattices were determined from three independent runs. Only one system was simulated for $N = 256$ and $N = 512$.

3.1. Stationary rod

It is instructive to consider the process in which the rod is not permitted to move and thus acts as a *fixed* obstacle to monomer motion. Simulating this case, we determined the probability $P_{\text{stat}}(L)$ that all of the sites immediately to the right of the rod were

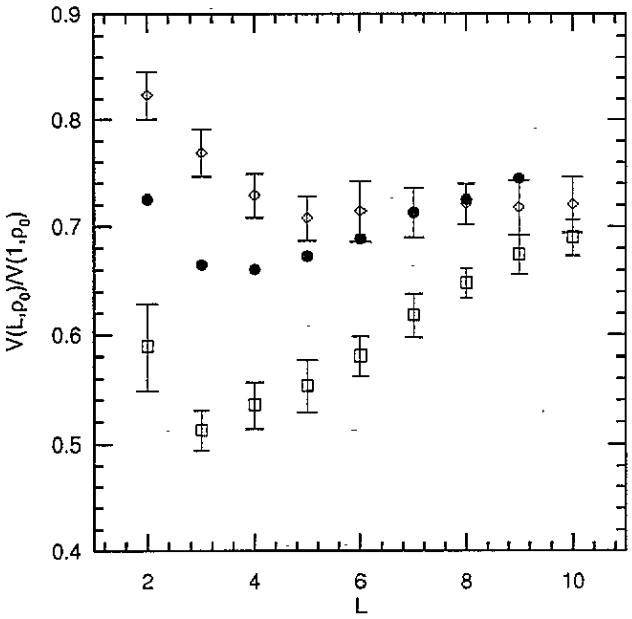

Figure 3. (*a*) Normalized velocity as a function of rod length for $\rho = 0.25(\Diamond)$, $\rho = 0.50(\bullet)$, $\rho = 0.75$ ($\Box$). $N = 128$, $b_\perp = 0.25$ and $b_\parallel = 0.50$. (*b*) Velocity as a function of rod length for $\rho = 0.50(\bullet)$; $N = 128$, $b_\perp = 0.25$ and $b_\parallel = 0.50$.

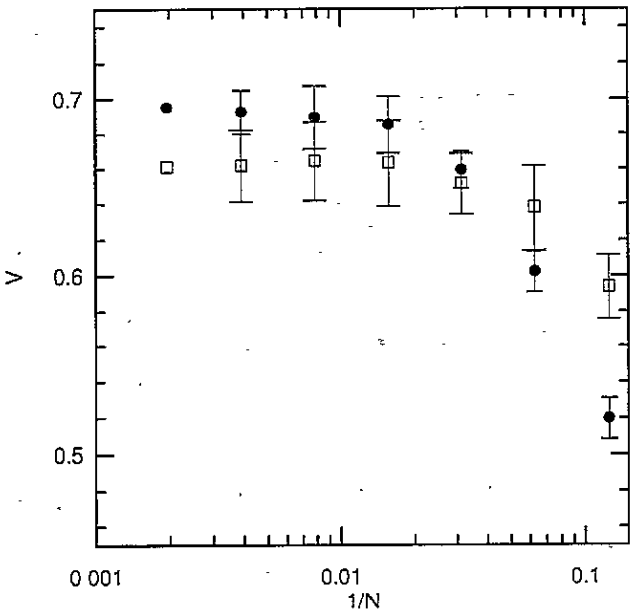

Figure 4. Finite-size effects: velocity as a function of inverse lattice size for rod lengths $L = 6$ ($\bullet$) and $L = 3$ ($\Box$).

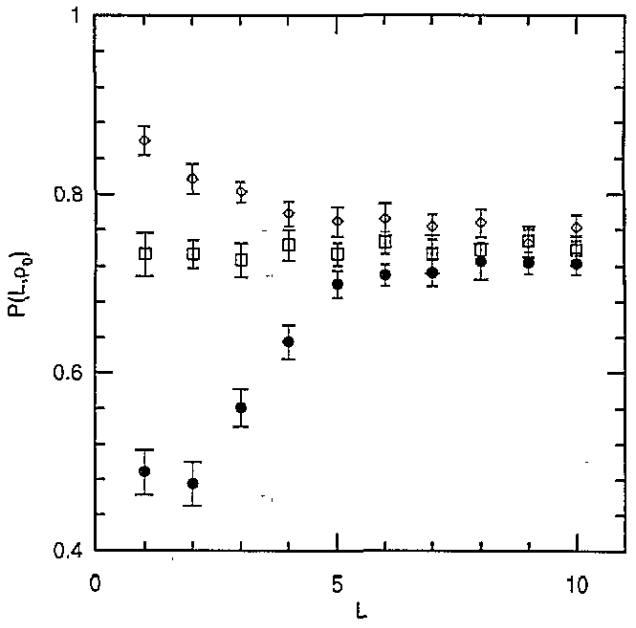

Figure 5. Stationary rod. Probability that all sites to the right are unoccupied ($N = 128$). 10 000 MCS to equilibrate. Averages taken over next 50 000 MCS.

simultaneously unoccupied. We found behaviour for $P_{\text{stat}}(L)$ similar to what we observed in the moving rod case. In figure 5 we show $P_{\text{stat}}(L)$ for three different monomer densities ρ_0. The system size was 128×128, and the jump rates were the same as before. Note that the asymptotic behaviour of $P_{\text{stat}}(L)$ seems to be be density-independent!

For a moving rod the normalized velocity, also seemed to become density-independent asymptotically in L (figure 3). This suggests that the long rods, whether stationary or moving, distort the local monomer profile to a state which is ρ_0-independent.

In the case of a stationary rod, when the monomer density $\rho_0 = 0.5$, there is a special symmetry in the dynamics of particles and holes. The average density of holes at a site is equal to the average density of particles at the site reflected through the rod axis:

$$\langle \rho(i\hat{e}_1 + j\hat{e}_2) \rangle_{ss} = 1 - \langle \rho(-i\hat{e}_1 + j\hat{e}_2) \rangle_{ss} \tag{8}$$

where the angle brackets $\langle\rangle_{ss}$ indicate a steady-state average. Therefore, the average site density along the line containing the rod axis is $\rho_0 = 0.5$. In the stationary state density profiles we see this behaviour for $\rho_0 = 0.5$ (figure 6(a)) while for densities $\rho_0 \neq 0.5$, there is a 'wing-like structure' in the density pattern (figure 6(b)) with a 'wing-like' region of lower (than ρ_0) density to the right of the rod. If the monomer density $\rho_0 < 0.5$, there is a 'wing-like' region of higher (than ρ_0) density to the right of the rod (figure 6(c)).

4. Macroscopic equations

Our simulations have presented us with an interesting and unexpected dependence of the density in front of the rod as a function of its length. We now describe some related continuum models whose behaviour is quite similar to that of P_{stat} for the particle model.

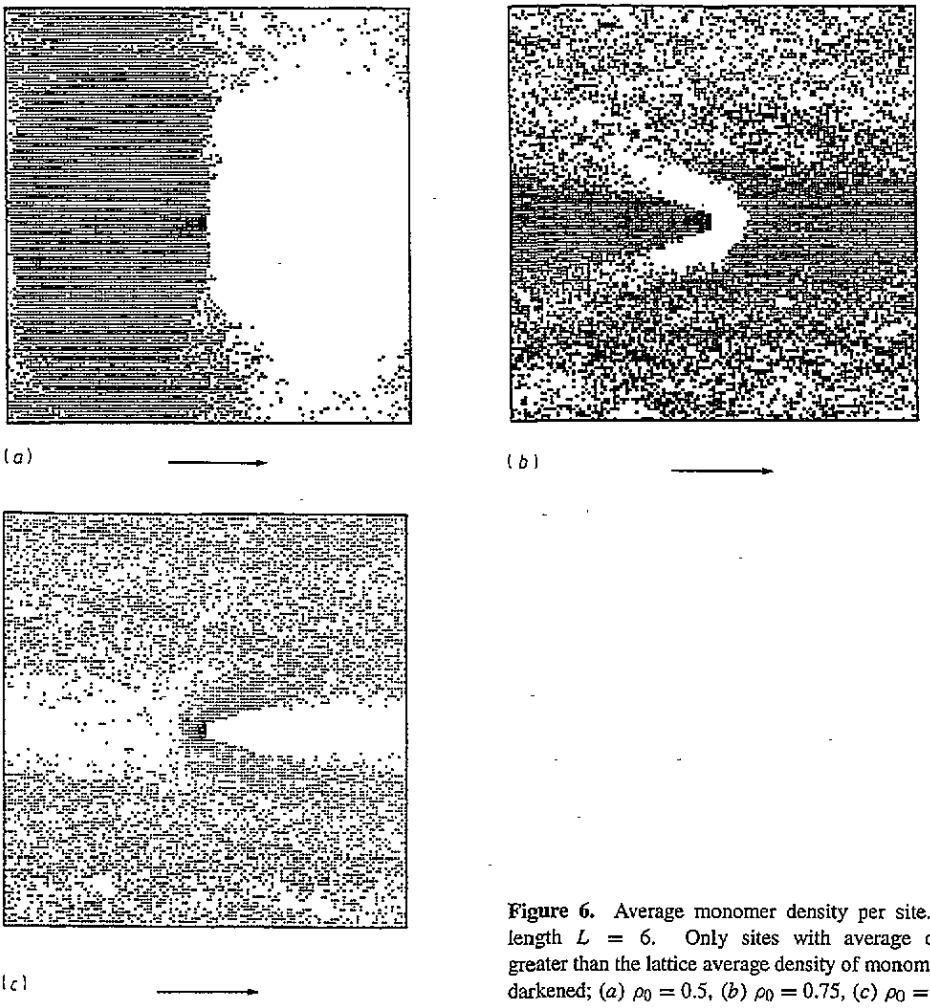

Figure 6. Average monomer density per site. Rod length $L = 6$. Only sites with average density greater than the lattice average density of monomers are darkened; (*a*) $\rho_0 = 0.5$, (*b*) $\rho_0 = 0.75$, (*c*) $\rho_0 = 0.25$.

4.1. Macroscopic Equations

Consider the continuum problem of driven diffusive flow past an impenetrable obstacle in two dimensions. We choose a disk of radius 1 centred at the origin, since for this geometry the problem is exactly soluble. In the limit of low particle density, the particle current is composed of two terms: a linear diffusion term $-D\nabla\rho$ and a drift term $\hat{e}_1 v\rho$. Therefore, the total current is given by

$$J = -D\nabla\rho + \hat{e}_1 v\rho\,. \tag{9}$$

and using the equation of continuity

$$\frac{\partial\rho}{\partial t} = -\nabla \cdot J \tag{10}$$

we have

$$\frac{\partial\rho}{\partial t} = D\Delta\rho - v\frac{\partial\rho}{\partial x}\,. \tag{11}$$

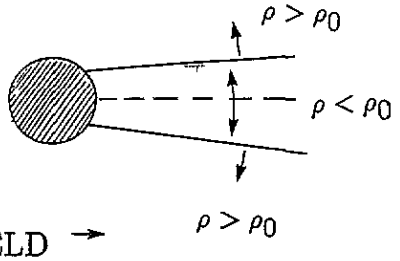

Figure 7. Map of density ρ for linearized diffusive drift past a disk. Profiles are obtained from the exact solution of Philip *et al* [14].

The boundary condition prohibiting a particle current from crossing the disk surface is, according to equation (9),

$$D\frac{\partial \rho}{\partial r}\bigg|_{r=1} = v\rho\cos\theta \tag{12}$$

at the surface. Here θ is the angle measured from the positive x-axis.

Note that while our particle model, has an upper bound on the particle density per site, $0 \leqslant \rho \leqslant 1$, the continuum (11), (12) impose no such condition. Nevertheless, we expect equations (11), (12) to provide a qualitative understanding of the density profile when the particle density is low, $\rho \ll 1$ and the drift is weak relative to the diffusion $v/D \ll 1$.

Equations (11), (12) were recently studied in the context of unsaturated flow of ground water past obstacles by Philip *et al* [14] and solved exactly in the form of an infinite series

$$\frac{\rho(r,\phi)}{\rho_0} = 1 + 4e^{(vr/2D)\cos\phi}\left(\sum_{j=1}^{\infty}\frac{jI_j(v/2D)}{K_j(v/2D)}K_0(vr/2D)\right.$$
$$\left. + \sum_{n=1}^{\infty}(-1)^j K_n(vr/2D)\cos n\phi\left[\frac{nI_n(v/2D)}{K_n(v/2D)} + 2\sum_{j=n+1}^{\infty}\frac{jI_j(v/2D)}{K_j(v/2D)}\right]\right). \tag{13}$$

The qualitative features of the density profile (figure 7) resemble those observed in the simulations of monomer flow past a stationary obstacle (figure 6(*b*)). Namely, to the right of the disk there is a 'shadow region' with particle densities lower than the asymptotic density: $\rho(r,\phi)/\rho_0 < 1$. There are lobes which extend around the disk with a higher density, and there is a boundary layer region of much higher density immediately to the left.

4.1.1. Discretized equations. We have also analysed a continuous-density, correlationless version of the particle process. In this case we replace the Boolean variable $\eta(x)$, representing the particle occupation number, by a continuous density $\rho(x)$, $0 \leqslant \rho(x) \leqslant 1$. At each time step there is a flux J of density out of a site x to each of its neighbours. This flux consists of two contributions. The first

$$J_{\text{drift}} = v\rho(1-\rho)\hat{e}_1\,. \tag{14}$$

results from the drift and the second

$$J_{\text{diff}} = D\nabla_\perp\rho \tag{15}$$

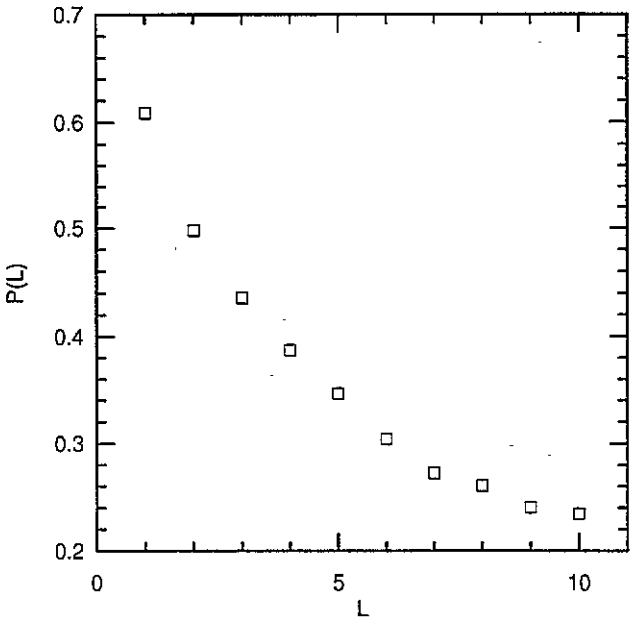

Figure 8. $P_{\text{stat}}(L)$ for the linearized discrete equation with $D = 0.25$, $\rho_0 = 0.5$, and $v = 0.50$, $N = 128$.

a diffusive flux perpendicular to the drift. This process arises from a naive finite differencing of Burgers' equation

$$\frac{\partial \rho}{\partial t} = D\frac{\partial^2 \rho}{\partial y^2} - v\frac{\partial \rho(1-\rho)}{\partial x}. \tag{16}$$

We further impose the condition that there can be no flux through a length L (rod) obstacle centred on the origin and oriented perpendicular to the drift. In addition to the nonlinear drift we have also considered a linearized version:

$$J_{\text{drift}} = v\rho\hat{e}_1 . \tag{17}$$

Of interest are the steady-state local densities at sites immediately to the right of the obstacle. We relate these densities to the probability that all of these sites are simultaneouly unoccupied through

$$P_{\text{stat}}(L) = \prod_{\text{sites to right of rod}} (1 - \rho(x)) . \tag{18}$$

This approach assumes no correlations between monomers in the actual particle process.

In figure 8 we show the results for the linear process. This was run on a 128×128 lattice with periodic boundary conditions in both directions. For comparison, we have set $D = 0.25$, the same as the perpendicular rates in the particle process, and $v = 0.5$. Note that $P_{\text{stat}}(L)$ is monotonically decreasing in L.

In figure 9 we plot $P_{\text{stat}}(L)$ as a function of rod length for the discrete nonlinear process with initial densities $\rho_0(x) = 0.25$, 50 and 0.75 with $D = 0.25$ and $v = 0.50$. The results look very similar to those obtained from simulations of the particle process as seen in figure 5.

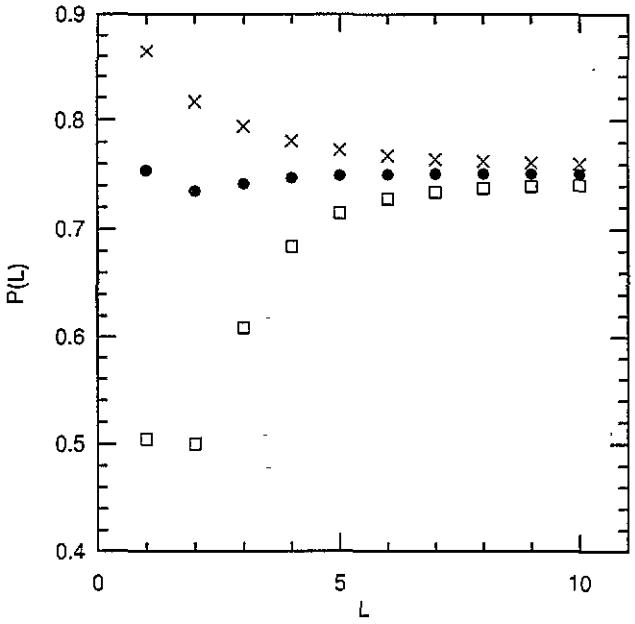

Figure 9. $P_{\text{stat}}(L)$ for the nonlinear discrete equation with $D = 0.25$, $v = 0.50$. $\rho_0 = 0.25$ (×); $\rho_0 = 0.50$ (•), and $\rho_0 = 0.75$ (□), $N = 256$.

5. Summary

We have studied an interacting particle model with two kinds of particles on a lattice. While some of its properties were expected and are well understood (e.g. flow patterns and convergence to Brownian motion) others were surprising and remain unexplained except at a heuristic level.

The anomalous behaviour of the rod velocity, $V(L)$ and probability that all sites to the right of the rod are unoccupied P_{stat} appears to be a result of the exclusion rule in the particle dynamics and the blocking effect of the rod. We have shown that steady-state values of the continuous density process reveal similar behaviour, so that the effect seems to have a hydrodynamic explanation. However, we have not shown that this is the appropriate hydrodynamic limit of our model. This remains an open problem.

Why P_{stat} is density-independent (and length-independent) for asymptotically long rods, is also an open problem. The anomalous behaviour appears to result from the fact that the blocking of long rods is primarily at the ends. Long rods create a larger depletion region (more holes) to the right of them. These holes are then driven to the left and replace particles near the edges. The longer the rod, the lower the density near the edges. Near the rod (for long rods) a density profile is established which is independent of the asymptotic density of monomers ρ_0.

Acknowledgments

This work was supported by AFOSR Grant AF-0115. FJA was also supported by a Rutgers University Excellence Fellowship and by the Department of Energy at Los Alamos LA-UR-93-1572. We thank M G Ancona, Z Cheng, G L Eyink, P Ferrari, P Garrido, S Janowsky,

J Keller, R Mainieri, P Rosenau, H Spohn, J Steif, H van Beijeren and S R S Varadhan for many fruitful discussions. FJA thanks S Chen and G D Doolen for their support at Los Alamos National Laboratory.

Appendix. Weak-field limit

Here we calculate the density profile of monomers where one site is blocked and the asymmetry in the jump rates, along the positive $\hat{e}_1$ axis, is weak. It is convenient to work in the language of spins $s = \pm 1$ using the relationship

$$s(x) = 2\eta(x) - 1 . \tag{A1}$$

We also translate the average monomer density ρ_0 into the net magnetization $m = 2\rho_0 - 1$. We then have the master equation

$$\frac{\partial \langle s(x) \rangle}{\partial t} = \sum_{|y-x|=1} \langle (s(y) - s(x))\, c(x, y; \mathbf{s}) \rangle \tag{A2}$$

with jump rates from x to y in the configuration $\mathbf{s}$

$$c(x, x \pm \hat{e}; \mathbf{s}) = \begin{cases} 1 & \text{if } \hat{e} \neq \pm\hat{e}_1 \\ (1 \pm \epsilon/2)(s(x) - s(x \pm \hat{e})) & \text{if } \hat{e} = \hat{e}_1 \text{ and } x \neq 0, \mp\hat{e}_1 \\ 0 & \text{in other cases.} \end{cases}$$

This gives

$$\begin{aligned} \frac{\partial \langle s(x) \rangle}{\partial t} = {} & \big\langle (s(x + \hat{e}_1) - s(x))(1 - \epsilon/2)(s(x + \hat{e}_1) - s(x)) \big\rangle (1 - \delta_{x,0})(1 - \delta_{x,-\hat{e}_1}) \\ & + \big\langle (s(x - \hat{e}_1) - s(x))(1 - \epsilon/2)(s(x) - s(x - \hat{e}_1)) \big\rangle (1 - \delta_{x,0})(1 - \delta_{x,\hat{e}_1}) \\ & + \sum_{\hat{e} \perp \hat{e}_1} \big\langle (s(x - \hat{e}) - s(x))(s(x + \hat{e}) - s(x)) \big\rangle (1 - \delta_{x,0})(1 - \delta_{x,\hat{e}}) . \end{aligned} \tag{A3}$$

The steady-state ($\partial \langle s \rangle / \partial t = 0$) solution of this equation is to zeroth order in ϵ

$$\langle s(x) \rangle_0 = \delta_{x,0} + (1 - \delta_{x,0}) m \tag{A4}$$

i.e. the site at the origin always has spin up (occupied), while all other sites have average magnetization m (particle density $(m + 1)/2$).

To first order in ϵ we have

$$\begin{aligned} 0 = {} & (\Delta_\parallel + \Delta_\perp) \langle s(x) \rangle_1 + \big(\langle s(x) s(x + \hat{e}_1) \rangle_0 - \langle s(x) s(x - \hat{e}_1) \rangle_0 \big) \\ & + \sum_{\hat{e} \perp \hat{e}_1} \delta_{x,-\hat{e}} \langle s(-\hat{e}) \rangle_1 + \sum_{\hat{e} \perp \hat{e}_1} \delta_{x,\hat{e}} \langle s(\hat{e}) \rangle_1 - \delta_{x,0} \big(\langle s(\hat{e}_1) \rangle_1 + \langle s(-\hat{e}_1) \rangle \big) \\ & - \delta_{x,-\hat{e}_1} \big(m - 1 - \langle s(-\hat{e}_1) \rangle_1 \big) - \delta_{x,\hat{e}_1} \big(-m + 1 - \langle s(\hat{e}_1) \rangle_1 \big) . \end{aligned} \tag{A5}$$

Here $\Delta_\perp$ and $\Delta_\parallel$ are finite-difference Laplacians

$$\Delta_\perp s(x) = s(x + \hat{e}_2) - 2s(x) + s(x - \hat{e}_2) \tag{A6}$$

and

$$\Delta_{\|} s(x) = s(x + \hat{e}_1) - 2s(x) + s(x - \hat{e}_1) \tag{A7}$$

and $\langle s(x)\rangle_1$ denotes the first-order correction to the stationary $\langle s(x)\rangle$

$$\langle s(x)\rangle = \delta_{x,0} + (1 - \delta_{x,0})m + \epsilon\langle s(x)\rangle_1 + \cdots . \tag{A8}$$

We introduce the zeroth-order approximation to the two-point function

$$\langle s(x)s(x + \hat{e}_1)\rangle_0 = \delta_{x,0}(1 - m)m + \delta_{x,-\hat{e}_1}(1 - m)m + m^2 . \tag{A9}$$

After some algebra we find

$$\Delta\langle s(x)\rangle_1 = \delta_{x,0}(\langle s(\hat{e}_1)\rangle_1) + \delta_{x,-\hat{e}_1}(1 - m^2 + \langle s(-\hat{e}_1)\rangle_1) + \delta_{x,\hat{e}_1}(m^2 - 1 + \langle s(\hat{e}_1)\rangle_1) + \sum_{\hat{e}\perp\hat{e}_1}(\langle s(\hat{e})\rangle_1 + \langle s(-\hat{e})\rangle_1) . \tag{A10}$$

In this form the density perturbation $\langle s(x)\rangle_1$ resembles an electrostatic potential due to a point charge of strength $\langle s(\hat{e}_1)\rangle_1$ located at the origin and charges of strength $(1 - m^2 + \langle s(-\hat{e}_1)$, $(m^2 - 1 + \langle s(\hat{e}_1)\rangle_1)$, and $(\langle s(\hat{e})\rangle_1 + \langle s(-\hat{e})\rangle_1)$ one lattice unit from the origin in the lattice directions.

The problem simplifies considerably if we consider the special case of $\rho = \frac{1}{2}$ or equivalently $m = 0$. Then, due to particle–hole duality, we have the following:

$$\langle s(\hat{e})\rangle_1 = 0 \qquad \text{for } \hat{e} \perp \hat{e}_1 \tag{A11}$$

and

$$\langle s(-\hat{e}_1)\rangle_1 = -\langle s(\hat{e}_1)\rangle_1 . \tag{A12}$$

We are thus left with

$$\Delta\langle s(x)\rangle_1 = \delta_{x,-\hat{e}_1}(1 + \langle s(-\hat{e}_1)\rangle_1) + \delta_{x,\hat{e}_1}(-1 + \langle s(\hat{e}_1)\rangle_1) . \tag{A13}$$

The perturbed density profile behaves like a potential due to a dipole of charges. Namely,

$$\langle s(x)\rangle \approx \frac{\epsilon}{r^{d-1}} \cos\theta(-1 + \langle s(\hat{e}_1)\rangle_1) \qquad r \gg 1 . \tag{A14}$$

References

[1] Alexander F J and Lebowitz J L 1990 *J. Phys. A: Math. Gen.* **L375**
[2] Rosato A, Prinz F, Strandburg K J and Swendsen R H 1986 *Powder Technol.* **49** 59
[3] Rosato A, Strandburg K J, Prinz F and Swendsen R H 1987 *Phys. Rev. Lett.* **58** 1038
[4] Liggett T M 1985 *Interacting Particle Systems* (New York: Springer)
[5] Billingsley P 1971 *Weak Convergence of Measures: Applications in Probability* (Philadelphia: SIAM)
[6] Spohn H 1991 *Large Scale Dynamics of Interacting Particles: Texts and Monographs in Physics.* (Berlin: Springer); 1990 *J. Stat. Phys.* 59 1227
[7] Kipnis C and Varadhan S R S 1986 *Commun. Math. Phys.* **104** 1
[8] Kehr K W and Haus R 1987 *Phys. Rep.* **150** 263
[9] Kehr K W and Binder K 1984 *Application of the Monte Carlo Method in Statistical Physics* ed K Binder (Berlin: Springer)
[10] Sankey O F and Fedders P A 1976 *Phys. Rev.* B **15** 3586
[11] Nakazato K and Kitahara K 1980 *Prog. Theor. Phys.* **64** 2261
[12] Varadhan S R S, private communication
[13] DeMasi A, Ferrari P A, Goldstein S and Wick W D 1989 *J. Stat. Phys.* **55** 787
[14] Philip J R, Knight J H and Waechter R T 1989 *Water Resources Res.* **25** 16